ELSEVIER

Chemical Engineering Journal 112 (2005) 23–31

Chemical Engineering Journal

www.elsevier.com/locate/cej

Flow structures in the downer circulating fluidized bed

Xuesong Lu *, Songgeng Li, Lin Du, Jianzhong Yao, Weigang Lin, Hongzhong Li

Multi-phase Reaction Laboratory, Institute of Process Engineering, Chinese Academy of Sciences, Beijing 100080, PR China

Received 25 January 2005; received in revised form 3 June 2005; accepted 10 June 2005

Abstract

The flow structures in downers have been investigated by a micro-video and by analysis of local voidage signals in this work. The experiments of micro-video action shot were performed in a downer with an internal diameter of 0.09 m. The local voidage signals were collected in a downer with an internal diameter of 0.285 m. The micro-video action shot showed that there were particle-clustering phenomena in the downer and the clusters existed mainly in the form of floc and stick. Through wavelet analysis of local voidage signals, the cluster size and frequency were obtained. However, the probability density distributions of local voidage signals confirmed that the clusters in the downer were unstable and could not form a stable phase.

Keywords: Downer; Flow structure; Cluster

1. Introduction

The complex structures and its dynamic variation are the common characteristics of a complex multiphase system, causing the difficulties for the study and quantitatively description and project of the system. A downer reaction system belongs to this class of multiphase systems. Besides the common structures of the flow, the different phases (gas and solids) in a downer can aggregate to form also meso-scale structures. There are a dilute phase (more dispersed) and a cluster phase (more dense). These meso-scale structures can be affected by the system boundaries and by its own interactions forming complex macro-structures characterized by mean radial and axial solids distributions. Therefore, the study of these transient flow structures in downers can elucidate which mechanisms are important for the control of flow behaviors, and for the downer design, scale-up and overall control.

Many investigations have been performed to study the flow structures in downers. Yang et al. [1] showed that in a downer, the particle concentration was uniform in the radial direction except for the position near the wall, where a dense phase zone ($r/R = 0.86$–0.95) existed and the particle density was 2–3 times higher than that of bed center. Krol et al. [2] studied the cluster formation in down flow reactors by using a new optical sensor, the CREC-GS-Optic probe. They found that the solid evolved as strings of particles and the average cluster size was ranged from 2 to $6d_p$ with most probable string size of $3.5d_p$. Zhang et al. [3] presented that there existed particle clusters in the downer, but a stable cluster phase with solids fraction of $1\text{-}\varepsilon_{mf}$ was not observed. However, presently, the opinions on the existence of cluster in a downer are rather divergent. A definition of "cluster" in a detectable way is of great importance as well. Sharma [4] has proposed a criterion for detecting the starting and ending time of a cluster once it has been detected by the $2\sigma_s$ criterion of Soong et al. [5].

Nowadays, there are numerous studies on flow structures and clusters in risers [6–16]. Li et al. [9] first observed the clusters in the riser of CFB by using the micro-camera. Horio et al. [10–11] used the multiple laser-sheet techniques to observe the three-dimensional flow structures of dilute suspensions in the circulating fluidized bed. The cluster size and their velocity distributions were determined from the video image analysis. Using the high-speed video technique in combination with the laser sheet technique, Lackermeier et al. [12] visualized the local flow structure inside upper dilute zone of CFB and successfully obtained shapes and

* Corresponding author. Tel.: +86 10 62572591.
E-mail address: xslu@home.ipe.ac.cn (X. Lu).

1385-8947/$ – see front matter © 2005 Elsevier B.V. All rights reserved.
doi:10.1016/j.cej.2005.06.002

Nomenclature

d_p	particle diameter (m)
D_{cluster}	cluster size (m)
$\overline{D}_{\text{cluster}}$	average cluster size (m)
f	cluster frequency at a certain point (1/s)
g	acceleration of gravity (m/s^2)
G_s	mass flow rate (kg/m^2 s)
i	ith cluster
l	bed length from the solids entrance (m)
n	cluster number
r	radial interval (m)
R	bed radial (m)
Re	Reynolds number
$t_{\text{c,after}}$	back peak time around cluster position in wavelet resolution signal (s)
$t_{\text{c,before}}$	former peak time around cluster position in wavelet resolution signal (s)
$t_{\text{c,end}}$	end time of cluster through an optical fiber (s)
$t_{\text{c,start}}$	start time of cluster through an optical fiber (s)
Δt_{cf}	time of cluster through a certain point (s)
$\overline{\Delta t}_{\text{cf}}$	average cluster falling time (s)
Δt_{whole}	whole time of time series (s)
Δt_1	cluster falling time through the point of an optical fiber (s)
Δt_2	cluster falling time from wavelet analysis (s)
U_{g}	gas velocity (m/s)
U_{t}	terminal velocity of particle (m/s)
U_{solid}	solid velocity (m/s)
V	output signal voltage of optical probe (V)

Greek letters

ε	voidage
ε_{mf}	voidage at minimum fluidization
$\overline{\varepsilon}_{\text{s}}$	mean solids holdup
μ	gas viscocity (Pa s)
ρ_{g}	gas density (kg/m^3)
ρ_{p}	particle density (kg/m^3)
σ_{s}	standard deviation of solid volume fraction

velocities of the flow structures. According to the heterogeneous structure consisting of a solid-rich dense phase (Cluster) and a gas-rich dilute phase, Li et al. [13] developed a comprehensive model of the energy-minimization multi-scale (EMMS) approach. Horio et al. [14] predicted the cluster size in circulating fluidized beds. Harris et al. [15] developed the correlations for predicting the properties of clusters of particles traveling near the riser wall such as cluster mean solid concentration, cluster size, cluster velocity, cluster shape, and time fraction of cluster appearance at the wall. Sharma et al. [16] studied the cluster characteristics, as determined by capacitance probe measurements of instantaneous local solid concentrations, and the results indicates the clusters can strongly affect operational characteristics, and the particle size, superficial gas velocity affects the duration time, occurrence frequency, time-fraction of existence and solid concentration in clusters. However, with gas–solids flow behaviors in downers researched further, the studies on the flow structure in a downer, especially with respect to clusters are attracting the researchers in the world [2–3,17]. This paper also focuses on experimentally studying the flow structures in a downer, attempting to explain the flow behavior from the viewpoint of the so-called "multi-scale approach" [18–20], which can be used to explain the "structure/interface" in a complex system.

2. Experimental

The experiments on flow structures in the downer were performed in two setups with different scales, shown schematically in Fig. 1. The voidage time series experiment was carried out in a large-scale downer. The micro-video action shot experiment was carried out in the smaller scale downer. The large scale indicates the larger diameter of downer tube and high solids circulation, and the small scale indicates the small diameter of downer tube and low solids circulation.

The large-scale downer system includes an elevator, a bag filter, a hopper, a screw, a fluidized bed feeder, a gas–solid diffuser and a tubular downer. The total height of the downer is 3.5 m with an inner diameter of 0.285 m, as shown in Fig. 1(a). The solid materials used in the experiment were glass beads with an average diameter of 57.6 μm and a density of 2500 kg/m^3. The smaller scale downer with an inner diameter of 0.09 m and a height of 8.2 m is shown in Fig. 1(b). The FCC particles with a density of 1350 kg/m^3 and an average diameter of 76 μm were used as the bed materials.

In a downer, the local gas–solids slip velocity is normally much higher than the terminal velocity of a single particle [21], which indicates that the particle clustering phenomena may exist. However, it is difficult to directly observe the individual cluster. In order to observe the micro scale gas–solids flow structures on line in the downers, the micro-video camera developed by the Institute of Process Engineering was used in the experiment. The measuring unit couples a microscopic lens with a new type CCD micro-camera. The optical glass rod and the compound lens sleeve can be inserted into the bed. When the compound lens is focused on a desired position in the downer, the shoot starts and the video of the local micro flow structure at the position can be logged in a computer. The schematic diagram of the video system is illustrated in Fig. 2.

If the cluster size is assumed to be the length of a cluster in the falling direction, Eq. (1) can be employed to estimate the cluster size

$$D_{\text{cluster}} = U_{\text{solids}} \Delta t_{\text{cf}} \tag{1}$$

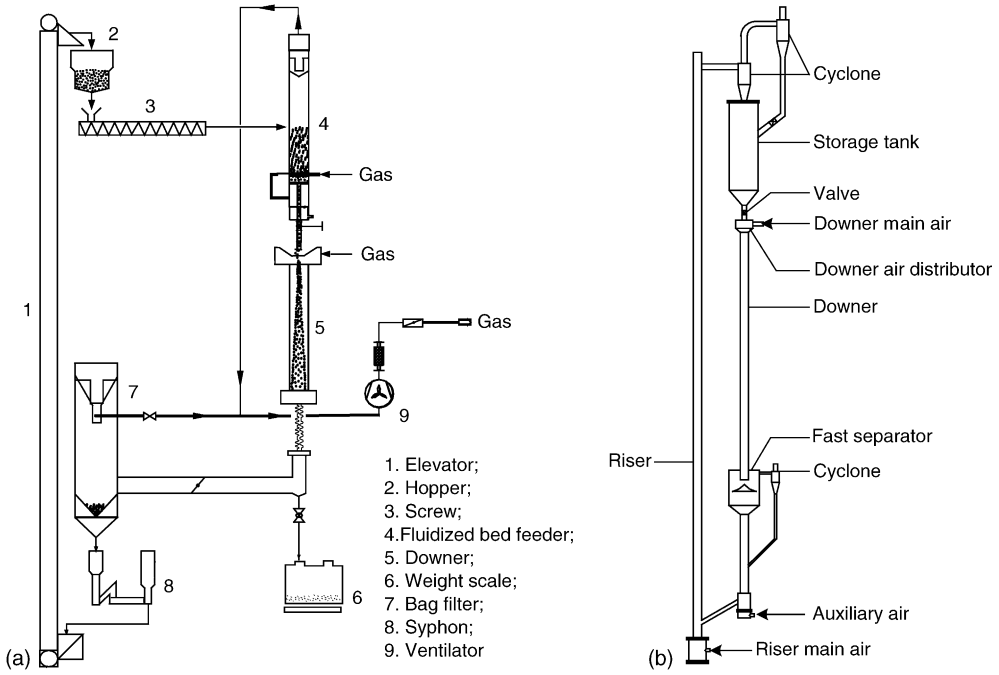

Fig. 1. Schematic diagram of experimental facilities.

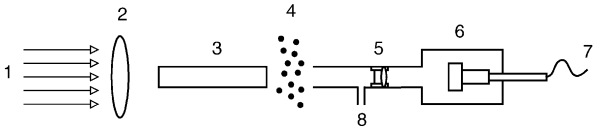

Fig. 2. Schematic diagram of the video system for micro gas–solid flow structures.

where $D_{cluster}$ represents the cluster size; U_{solid} the solids velocity; t_{cf} the time of cluster through a certain point.

The solids velocity and bed voidage can be measured by the double optical fiber probe system, which can simultaneously collect the local voidage data at two vertical points. In each probe, two beams of light, a reference light and a measuring light, were used. Through the cross-correlation calculation of two voidage signals, the delay time can be obtained. Thus, the solids velocity can be acquired from the interval of two optical fiber probes divided by the delay time. The principle of velocity measurement with double optical fiber probes is shown in Fig. 3. More details for the two probes and calibration method to determine the relationship between the output signal voltage and bed voidage are given by Li et al. [22], Zhang et al. [23], Zhu et al. [24] and Lin et al. [25]. In this experiment, the relationship of the output signal voltage and bed voidage can be described as

$$\varepsilon = 1 - 0.185V \quad (2)$$

3. Results and discussion

3.1. Cluster observation by the micro-video action shot in the downer

The images of clusters are shown in Figs. 4 and 5 at different conditions and different radial positions in the downer. l is the interval from the downer tube to the solids entrance, which locates below the air distributor shown in Fig. 1(b). The results of the micro-video action shot in Figs. 4 and 5 confirm that there exist the solid clustering phenomena in

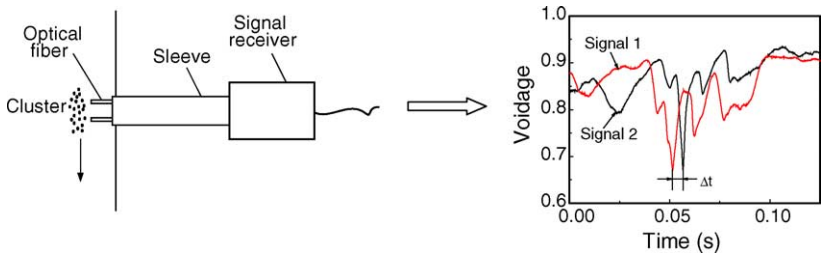

Fig. 3. Velocity measurement system of double optical fibers and its signals.

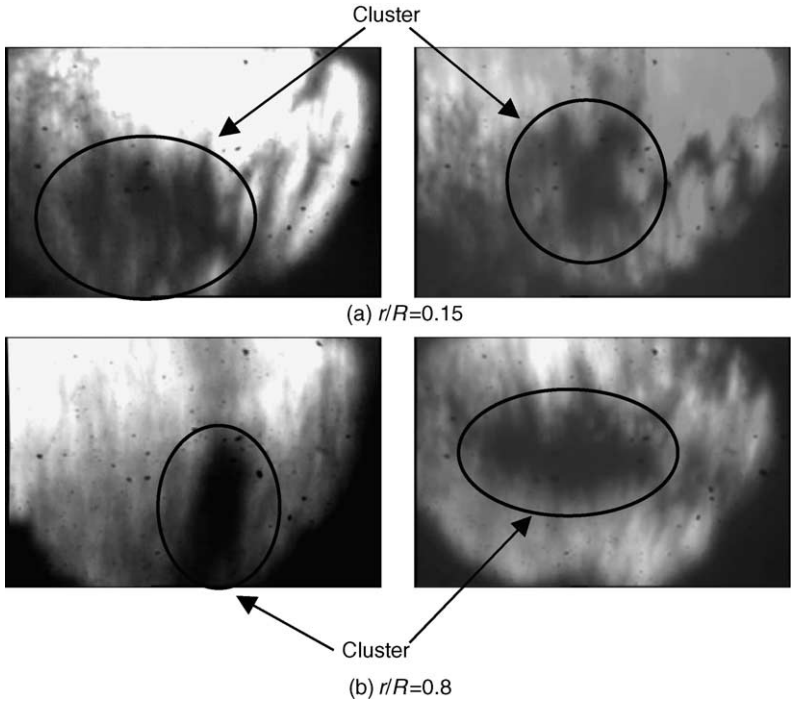

Fig. 4. Images of solid clusters in the downer $G_s = 75\ kg/(m^2\ s)$, $U_g = 2.1\ m/s$, $l = 4.5\ m$.

the downer. The configurations of clusters are anomalous and often in the form of floc and stick structures. However, the spherical and elliptic structures were sporadically observed. Near the bed wall with the relatively high density of particles, the occurrence probability of spherical clusters was higher than that in the bed center with the low particle concentration, and the size of cluster near the wall was also larger than that in the bed center. According to the observation, it is deduced that the clusters in the near wall zone may be more than that in the center zone, indicating that the cluster concentration in the center is lower than that near the wall.

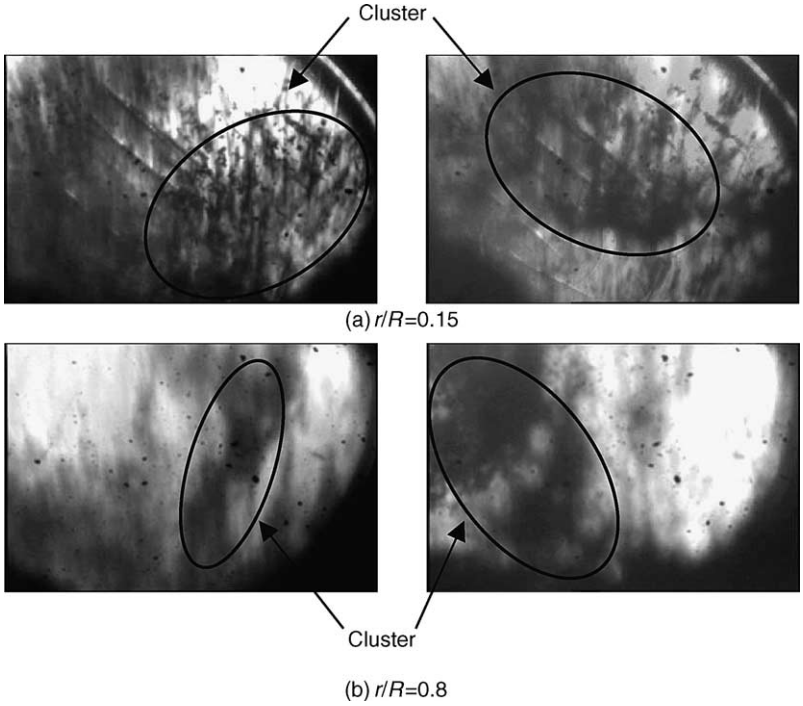

Fig. 5. Images of solid clusters in the downer $G_s = 50\ kg/(m^2\ s)$, $U_g = 1.4\ m/s$, $l = 4.5\ m$.

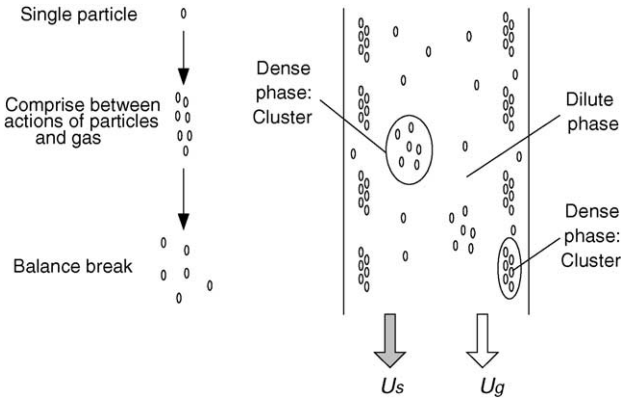

Fig. 6. Flow structures in the downer.

According to Li's multi-scale strategy [18–20], it is deduced that there should be a compromise of particle and gas interactive action in the downer. In the downer, the energy dissipated by the gas to suspend the particles tends to the minimum, and the solid down flow resistance inclines to the minimum as well. The impulsion of particles pursuing the maximum falling velocity induces particles gathering together to make the gas–solids slip velocity much higher than the terminal velocity of a single particle. At the same time, the clusters are broken under the function of the gas flow shear and minimum suspension energy. Thus, the flow structures in the downer can be assumed as those shown schematically in Fig. 6. In a word, the compromise of the above two behaviors should be the cause of the cluster formation and dispersion.

3.2. Average cluster size and frequency in the downer

Sharma [4] defined the starting time of a cluster for particle density signal, which is the time when its density exceeded the mean density satisfying the $2\sigma_s$ criterion. The ending time of a cluster was defined as the time when the density falls below $\overline{\varepsilon}_s$ after crossing the $2\sigma_s$ criterion. In this work, we attempt to gain the time of a cluster passing a position in the downer by wavelet analysis of voidage signals. The wavelet transform can provide information of a random signal with time and space. The original signal time-series can be resolved into multi-resolution signals with different frequency bands by wavelet transform. For example, the raw data can be decomposed into different scale signals and detail signals, and the original signal may be reconstructed from the information contained in the last scale signal and detail signals. With increasing the resolution, the amplitude of the resolved signals decreases for the pulse change (noise), increases for the gradual change and keeps constant for step variation of resolution-independent [26,27].

The experiments were performed at the condition with G_s of 0.56 kg/s without the solids dispersed gas (U_g = 0 m/s) to avoid the high electrostatic interface on the measurement. The data acquisition frequency was 20,000 Hz. The Mallat's pyramidal algorithm was used for one-dimensional orthonormal wavelet transform of a signal [28]. A typical set of results is shown in Fig. 7. It can be seen that when a cluster occurs, the voidage is decreased. The wavelet analysis illustrates that the multi-resolution signals manifest a negative peak followed by a positive peak in the "cluster" position, but other variations cannot cause obvious changes in their corresponding positions.

On the other hand, it is important for us to determine the cluster boundary surface because the solid concentration of the cluster in the downer is varied gradually from the bed zone to the cluster center zone. We deem that the solid

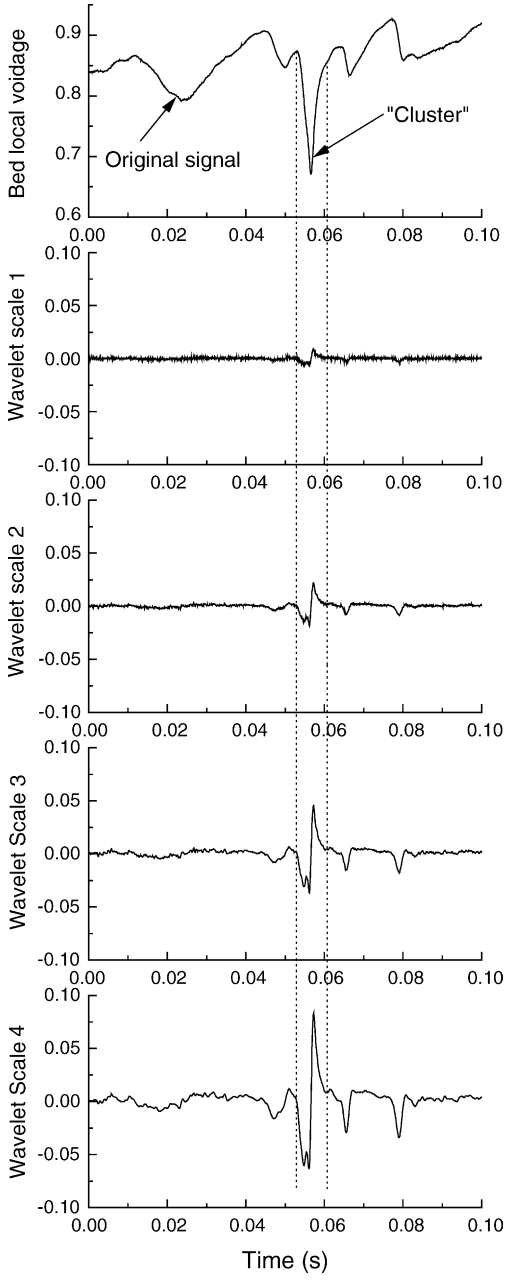

Fig. 7. Characteristics of wavelet analysis of a voidage signal on a cluster.

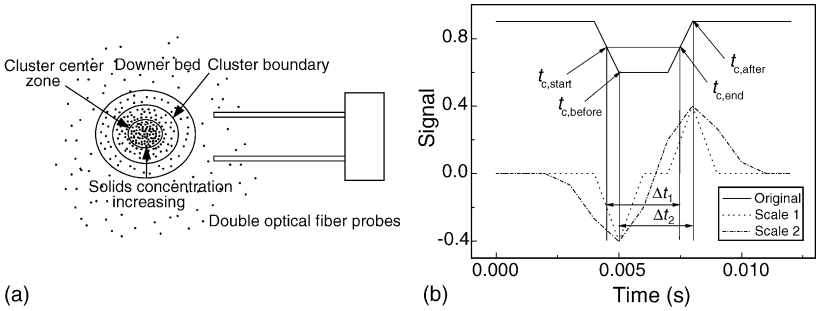

Fig. 8. Definition of cluster boundary and determination of the cluster falling time.

concentration around the boundary should not be regarded as the solid concentration of the bed, so in this paper, the cluster boundary surface is the position, in which the solid concentration is changed half from the concentration of the bed to that of the cluster center zone, as shown in Fig. 8(a). Thus, the cluster can differ distinctly from the bed solids.

Fig. 8(b) shows an example, in which a "cluster" variation in the original signal causes a positive peak and a negative peak in the resolution signals. According to the above definition of the cluster boundary, $t_{c,start}$, the start time of a cluster through an optical fiber, can be defined as the time when the solid concentration increases half from the concentration of the bed to that of the cluster center zone. Accordingly, $t_{c,end}$, the end time of a cluster through an optical fiber, can be defined as the time when the solid concentration decrease half from the concentration of the cluster center zone to that of the bed. At the same time, $t_{c,before}$ is the time of the fore peak around cluster position in the wavelet resolution signal, corresponding to the time when the solid concentration increased to that of cluster center zone. Accordingly, $t_{c,after}$ is the time of the hind peak around cluster position in the wavelet resolution signal, corresponding to the time when the solid concentration decreased to that of the bed.

Thus, the period of a cluster passing through the tip of the optical fiber probe is

$$\Delta t_1 = t_{c,end} - t_{c,start} \tag{3}$$

and the time between two peaks in resolution signals is

$$\Delta t_2 = t_{c,after} - t_{c,before} \tag{4}$$

From Fig. 8(b), it can be seen obviously

$$t_{c,before} - t_{c,start} = t_{c,after} - t_{c,end} \tag{5}$$

The relationship between Δt_1 and Δt_2 is

$$\Delta t_2 = \Delta t_1 = \Delta t_{cf} \tag{6}$$

where Δt_{cf} is the period of the cluster passing through the probe tip, which can be obtained by

$$\Delta t_{cfi} = t_{ci,after} - t_{ci,before} \tag{7}$$

The average time can be calculated from the following equation

$$\Delta \bar{t}_{cf} = \frac{\sum_{i=1}^{i=n} \Delta t_{cfi}}{n} \tag{8}$$

The average cluster size is defined by

$$\bar{D}_{cluster} = U_{solid} \Delta \bar{t}_{cf} \tag{9}$$

The average frequency of clusters appeared at a certain point for time series is

$$f = \frac{n}{\Delta t_{whole}} \tag{10}$$

To study the flow structure in a downer using the above-described procedure, the cluster characteristics with the bed length, which is the interval from the particle entrance to the measuring point, were investigated. In order to increase the reliability, 116,000 points of the signal were used for analyzing. Fig. 9 shows the results of the measurement and calculation.

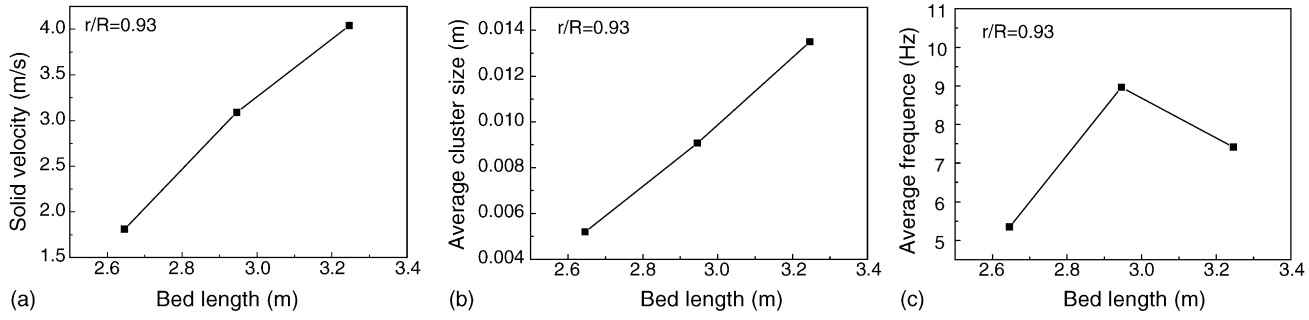

Fig. 9. Solid velocity, average cluster size and average frequency in the downer ($r/R = 0.93$).

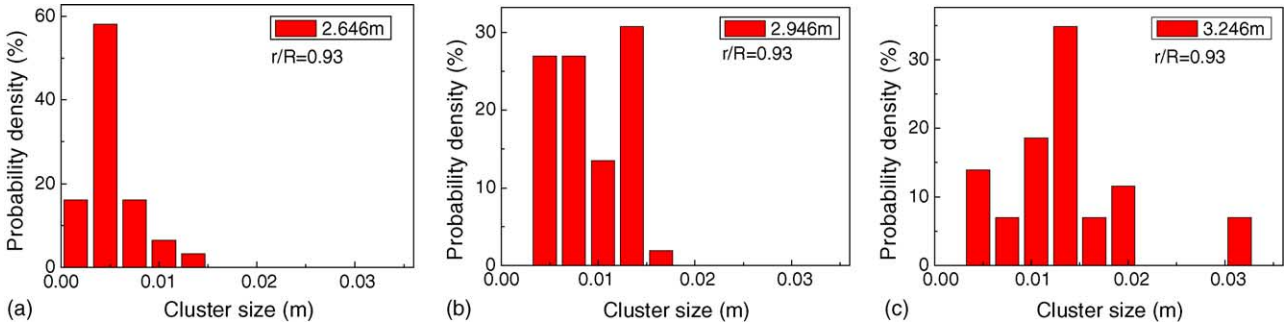

Fig. 10. Probability density of cluster sizes at different bed lengths.

In order to compare the velocity of a cluster with the terminal velocity of a single particle, Eq. (11) is used to determine the flow type of a single particle at the terminal velocity

$$Re_t = \frac{d_p^3}{18\mu^2}(\rho_p - \rho_g)\rho_g g = \frac{K^3}{18} \quad (11)$$

When $\rho_g = 1.20\,kg/m^3$, $\rho_p = 2500\,kg/m^3$, $d_p = 57.6\,\mu m$ and $\mu = 1.81 \times 10^{-5}$ Pa s, K is equal to 2.57 due to Eq. (11). Because of $K < 2.62$, the flow of the particle is in the Stokes region. Thus, Eq. (12) can be used to calculate the terminal velocity of a single particle, which is equal to 0.25 m/s.

$$U_t = \frac{d_p^2}{18\mu}(\rho_p - \rho_g)g \quad (12)$$

The results of solid velocity measurement in Fig. 9(a) show that the solid velocity at the measurement point in the downer is more than the terminal velocity of a single particle, which indicates that the particle clustering phenomena should exist. Through the wavelet analysis of voidage signals, the average cluster size and average frequency in the wall region ($r/R = 0.93$) as a function of the bed length are obtained as shown in Fig. 9(b) and (c). It is illustrated that the average cluster size increases with an increase of the bed length. However, the average frequency first increases with the bed length and declines slightly with a further increase of the bed length. The reason may be that as the bed length is increased, the particles tend to move toward the bed wall, and the particle concentration inclines a little, which induces the cluster size increasing. Thus, the formation of larger clusters causes the frequency decline.

Fig. 10 shows the probability density distribution of cluster sizes at different bed lengths. At the bed length of 2.646 m, the average cluster size is relatively small, and the distribution is concentrated. At the bed length of 2.946 m, the cluster sizes are relatively concentrated as well. At the bed length of 3.246 m, the cluster size varies in a wide range.

3.3. Probability density distribution of voidage signals in the downer

Liu [29] studied the distribution of the voidage probability density at different regimes of fluidization and revealed that there is a strong relationship between the distribution and the two-phase structure of fluidized bed. The curve of the voidage probability density is symmetric corresponding to the homogenous fluidized bed. It is because the bed is homogeneous in the time and spatial coordinates. Thus, the curve of the voidage probability density displays a rectangular distribution. When the fluidization is in the particulate expansion zone at a low fluid velocity, the curve of the probability density is of left steep. With increasing the velocity, the peak moves rightward, and left gradient is weakened. With a further increase of the fluid velocity, the curve becomes of right steep. When the bubbling fluidization starts, two phases (dense phase and bubble phase) co-exist, and the curve transits from a single peak to double peaks corresponding to the dense phase and bubble phase. In the fast fluidization, there are also two peaks representing the co-existence of the two phases, dense phase (cluster) and dilute phase. The mapping of the gas–solid flow regime by the distribution of the voidage probability density is shown in Fig. 11.

In this experiment, the results of the probability density curves of voidage signals at the radial position of $r/R = 0.93$ with different bed lengths and at the bed length of 3.246 m with different radial positions are shown in Fig. 12 and

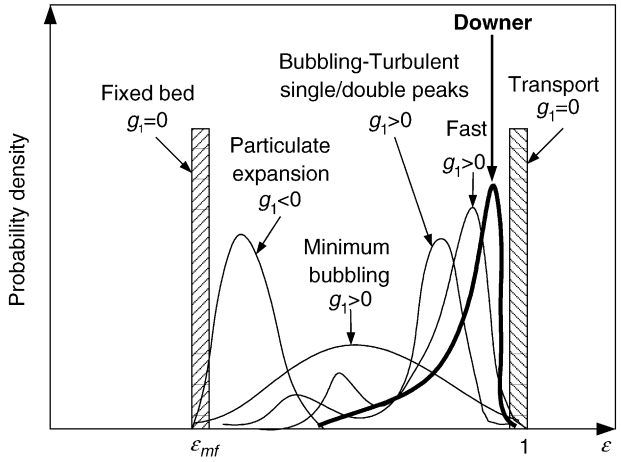

Fig. 11. Mapping of the gas–solid flow pattern by distribution of voidage probability density [29].

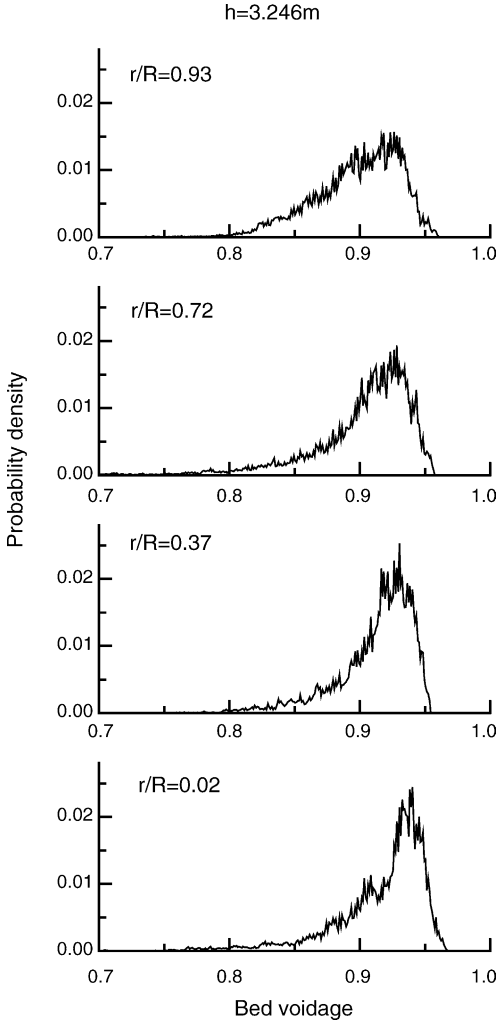

Fig. 12. Probability density distribution of voidage signals with different radial positions.

Fig. 13, respectively. It can be seen that the probability density curves of voidage signals are all single-peaked, which is different from the curves of bubbling bed and fast fluidized bed demonstrating the double-peak distribution caused by the obvious two-phase structure. Furthermore, in the fast-fluidized bed, the dynamic evolution and dissolution of clusters is one of important characteristics [30]. According to the characteristics of the voidage probability density in Fig. 11, the single-peak voidage distribution in the downer in Fig. 12 and Fig. 13 indicates that only one phase may exist in the downer, meaning that the particles may not form a stable cluster. The probability density curve in the bed center ($r/R = 0.02$) is narrow, while the distribution curve in the near-wall zone ($r/R = 0.93$) is relatively wide. It is because the random alternative changes of the dense and dilute solids concentration are increased in the wall zone with relatively high particle concentrations. The shapes of curves in the same radial position at different bed lengths are similar.

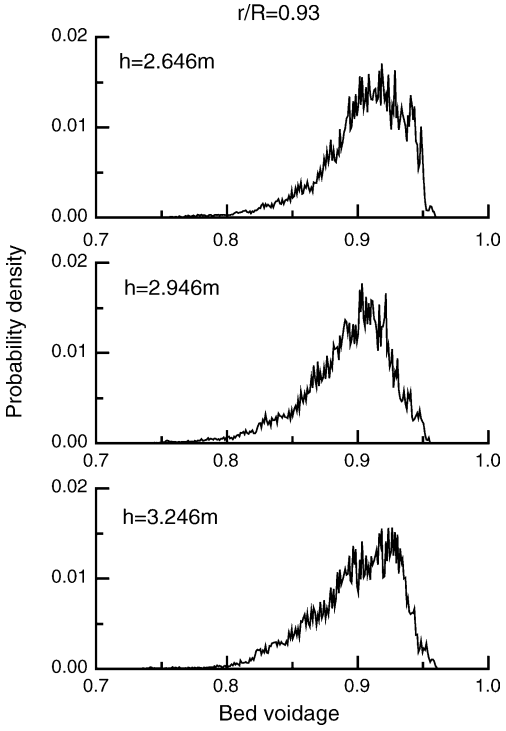

Fig. 13. Probability density distribution of voidage signals with different bed length positions.

4. Conclusion

(1) The experiment of the micro-video action shot showed that there existed the particle clustering phenomena. The clusters in the downer were mainly in the form of floc and stick.
(2) The cluster size can be calculated from the solid velocity and time of a cluster passing a position in the downer. By the cross-correlation and wavelet analysis of local voidage signals, the average cluster size and frequency as a function of bed length were obtained. The results showed that the cluster size and frequency in the downer were changed with different bed heights.
(3) The probability density distributions of local voidage signals in the downer exhibited only a single peak, which may indicate that only a single phase existed in the downer. The cluster in the downer observed by the micro-video action shot may be unstable with fast evolving and dissolving processes.

Acknowledgments

The authors gratefully acknowledge the financial support from the National Natural Science Foundation of China (Project No. 20221603 and 90210034), the National Basic Research Program (Project No. 2004CB719704) and Hi-Tech R&D program of China (Project No. 2003AA514023).

References

[1] Y.L. Yang, Y. Jin, Z.Q. Yu, et al., Paritcle flow pattern in a dilute concurrent upflow and down flow circulating fluidized bed, in: M. Kwauk, M. Hasatani (Eds.), Fluidization'91: Science and Technology, Science Press, Beijing, 1991, pp. 66–75.

[2] S. Krol, A. Pekediz, H. De Lasa, Particle clustering in down flow reactors, Powder Technol. 108 (2000) 6–20.

[3] Minghui Zhang, Zhen Qian, Hao Yu, et al., Analysis of flow structure in large-scale circulating fluidized beds, J. Chem. Ind. Eng. (China) 54 (2) (2003) 182–187.

[4] A.K. Sharma, Transient studies in fast-fluidized beds, Doctoral Dissertation, Lehigh University, USA, 2000.

[5] C.H. Soong, K. Tuzla, J.C. Chen, The identification of particle clusters in circulating fluidized bed, in: A.A. Avidan (Ed.), Circulating Fluidized Bed IV, Engineering Foundation, New York, 1993, pp. 615–620.

[6] Y. Li, M. Kwauk, The dynamics of fast fluidization, in: J.R. Grace, J.M. Matsen (Eds.), Fluidization III, Plenum Press, New York, 1980, pp. 537–544.

[7] M. Horio, R. Clift, A note on terminology: 'cluster' and 'agglomerates', Powder Technol. 70 (1992) 196.

[8] C.M.H. Brereton, J.R. Grace, Microstructural aspects of the behavior of circulating fluidized beds, Chem. Eng. Sci. 48 (1993) 2565–2572.

[9] H. Li, Y. Xia, Y. Tung, M. Kwauk, Micro-visualization of clusters in a fast fluidized bed, Powder Technol. 66 (1991) 231–235.

[10] M. Horio, H. Kuroki, Three-dimensional flow visualization of dilutely dispersed solids in bubbling and circulating fluidized beds, Chem. Eng. Sci. 49 (1994) 2413–2421.

[11] M. Tsukada, M. Ito, H. Kamiya, M. Horio, Three-dimension imaging of particle clusters in dilute gas–solid suspension flow, Can. J. Chem. Eng. 75 (1997) 466–470.

[12] U. Lackermeier, J. Rudnick, J. Werther, A. Bredebusch, H. Burkhardt, Visualization of flow structures inside a circulating fluidized bed by means of laser sheet and image processing, Powder Technol. 114 (2001) 71–83.

[13] J.H. Li, C.L. Cheng, Z.D. Zhang, J. Yuan, A. Nemet, F.N. Fett, The EMMS model: It's application, development and updated concepts, Chem. Eng. Sci. 54 (1999) 5409–5425.

[14] M. Horio, M. Ito, Prediction of cluster size in circulating fluidized beds, J. Chem. Eng. Jpn. 30 (4) (1997) 691–697.

[15] A.T. Harris, J.F. Davidson, R.B. Thorpe, The prediction of particle cluster properties in the near wall region of a vertical riser, Powder Technol. 127 (2) (2002) 128–143.

[16] A.K. Sharma, K. Tuzla, J. Matsen, J.C. Chen, Parametric effects of particle size and gas velocity on cluster characteristics in fast fluidized beds, Powder Technol. 111 (2000) 114–122.

[17] K. Tuzla, A.K. Sharma, J.C. Chen, T. Schiewe, K.E. Wirth, O. Molerus, Transient dynamics of solid concentration in downer fluidized bed, Powder Technol. 100 (1998) 166–172.

[18] W. Ge, J.H. Li, Physical mapping of fluidization regimes-the EMMS approach, Chem. Eng. Sci. 57 (2002) 3993–4004.

[19] J.H. Li, M. Kwauk, Exploring complex systems in chemical engineering-the multi-scale methodology, Chem. Eng. Sci. 58 (2003) 521–535.

[20] J.H. Li, J.Y. Zhang, W. Ge, X.H. Liu, Multi-scale methodology for complex systems, Chem. Eng. Sci. 59 (2004) 1687–1700.

[21] C. Cao, Y. Jin, Z. Yu, et al., The gas–solid velocity profiles and slip phenomenon in a courrent down flow circulating fluidized bed, in: A.A. Avidan (Ed.), Circulating fluidized bed technology IV (1993) 406–413.

[22] Hongzhong Li, Qingshan Zhu, Hua Liu, Yufeng Zhou, The cluster size distribution and motion behaviors in a fast fluidized bed, Powder Technol. 84 (4) (1995) 241–246.

[23] H. Zhang, P.M. Johnston, J.-X. Zhu, et al., A novel calibration procedure for a fiber optic solids concentration probe, Powder Technol. 100 (1998) 260–272.

[24] J.-X. Zhu, G.-Z. Li, S.-Z. Qin, et al., Direct measurements of particle velocities in gas–solids suspension flow using a novel five-fiber optical probe, Powder Technol. 115 (2001) 184–192.

[25] Q. Lin, F. Wei, Y. Jin, Transient density signal analysis and two-phase micro-structure flow in gas–solids fluidization, Chem. Eng. Sci. 56 (2001) 2179–2189.

[26] X.S. Lu, H.Z. Li, Wavelet analysis of pressure fluctuation signals in a bubbling fluidized bed, Chem. Eng. J. 75 (1999) 113–119.

[27] Jinqiang Ren, Jinghai Li, Wavelet analysis of dynamic behavior in fluidized beds, in: L.T. Fan, T.M. Knowlton (Eds.), Fluidization IX, 1998, pp. 629–636.

[28] Qianqing Qin, Zongkai Yang, Practical Wavelet Analysis, Xi'an Xidian University Press, 1995, pp. 25–27 (in Chinese).

[29] D.J. Liu, Fluidization of supercritical fluid, Doctoral dissertation, Institute of Chemical Metallurgy, CAS, Beijing, 1994.

[30] Linna Wang, Multi-scale mass transfer model and experimental validation for heterogeneous gas–solid two-phase flow, Doctoral dissertation, Institute of Process Engineering, CAS, Beijing, 2002.